WORKSHOP: A previsão numérica do tempo em Portugal: estado da arte e novos desafios

Instituto de Ciências da Terra
Institute of Earth Sciences

On the influence of Sun-Earth geometry and atmospheric variables on the predictions of solar global irradiation (GHI) obtained from the ECMWF model

Sara Pereira, Paulo Canhoto, Rui Salgado and Maria João Costa

Data

ECMWF
EUROPEAN CENTRE FOR MEDIUM RANGE WEATHER FORECASTS

Experimental data:

- Évora (May 13 2015 to November 15 2016): Kipp & Zonen CM6B pyranometer
- Sines (July 21 2015 to November 15 2016): LI-COR Li-200R pyranometer
- Cabo da Roca and Penhas Douradas (July 21 2015 to November 15 2016): Kipp & Zonen CM11 pyranometer, IPMA

S. Pereira, P. Canhoto, and R. Salgado, "Spatial and temporal downscaling of solar global radiation and mean air temperature from weather forecast data - an introductory numerical study and validation," in *Workshop On Earth Sciences 2016*, 2016, pp. 8–11.

Variable	ECMWF variable	Unit
Longitude	longitude	° East
Latitude	latitude	° North
Time step	step	h
Date	date	Days since 1900-01-01 00:00:00
Visibility	p3020	m
Cloud base height	cbh	m
Total column water	tcw	kg/m^2
Total cloud cover	tcc	0-1
10 metre U wind component	u10	m/s
10 metre V wind component	v10	m/s
2 metre temperature	t2m	K
2 metre dew point temperature	d2m	K
Surface solar radiation downwards	ssrd	J/m^2
Total column ozone	tco3	kg/m^2


Penhas Douradas
Cabo da Roca
Évora
Sines
Data SIO, NOAA, U.S. Navy, NGA, GEBCO
Image Landsat / Copernicus
Google Earth
Data das imagens: 14/12/2015 42°13'55.53"N 1°33'31.28"E elev 0 m altitude de visualização 3372.01 km

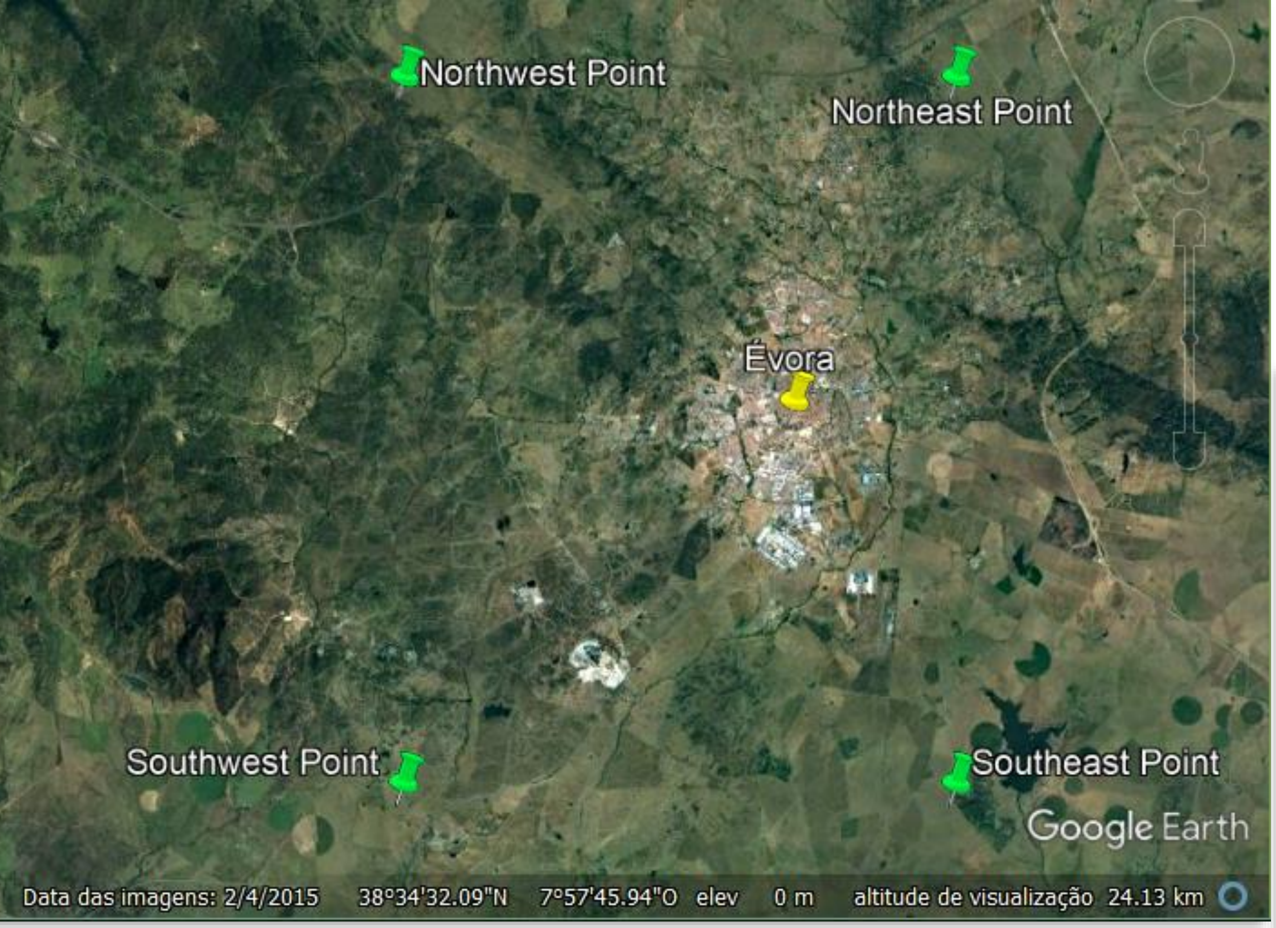
Northwest Point
Northeast Point
Évora
Southwest Point
Southeast Point
Google Earth
Data das imagens: 2/4/2015 38°34'32.09"N 7°57'45.94"O elev 0 m altitude de visualização 24.13 km

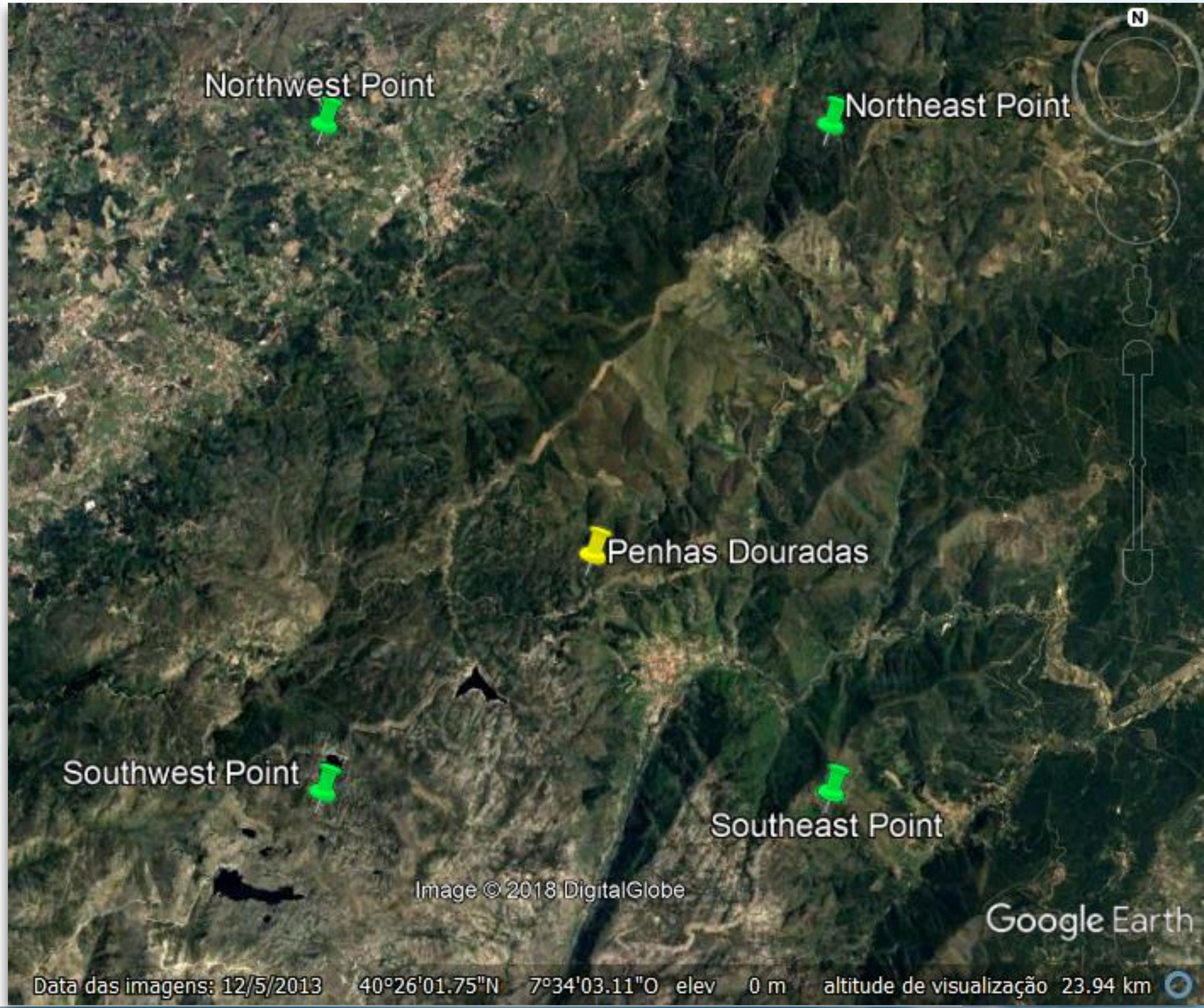
N
Northwest Point
Northeast Point
Penhas Douradas
Southwest Point
Southeast Point
Image © 2018 DigitalGlobe
Google Earth
Data das imagens: 12/5/2013 40°26'01.75"N 7°34'03.11"O elev 0 m altitude de visualização 23.94 km

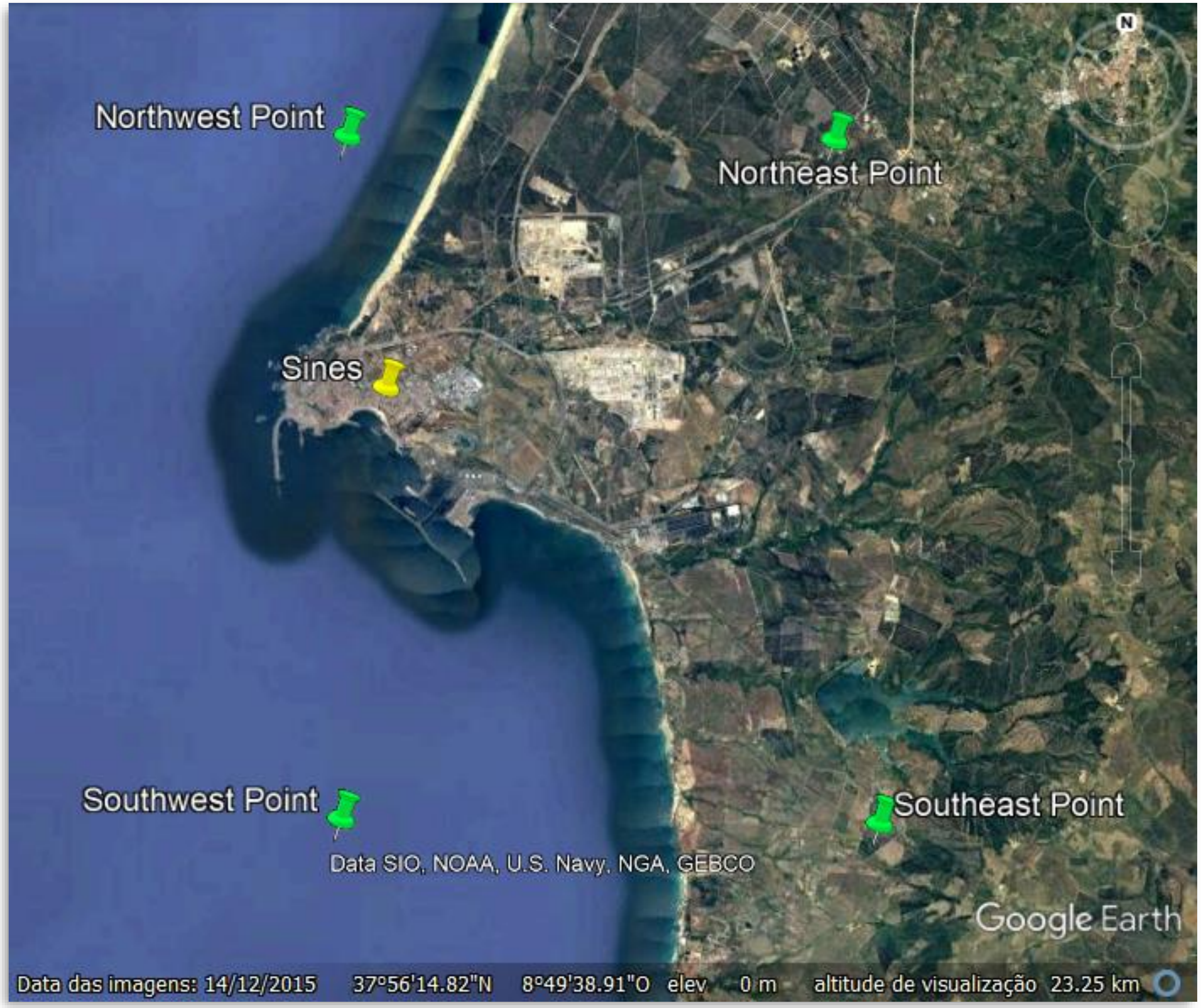
Northwest Point
Northeast Point
Sines
Southwest Point
Southeast Point
Data SIO, NOAA, U.S. Navy, NGA, GEBCO
Google Earth
Data das imagens: 14/12/2015 37°56'14.82"N 8°49'38.91"O elev 0 m altitude de visualização 23.25 km

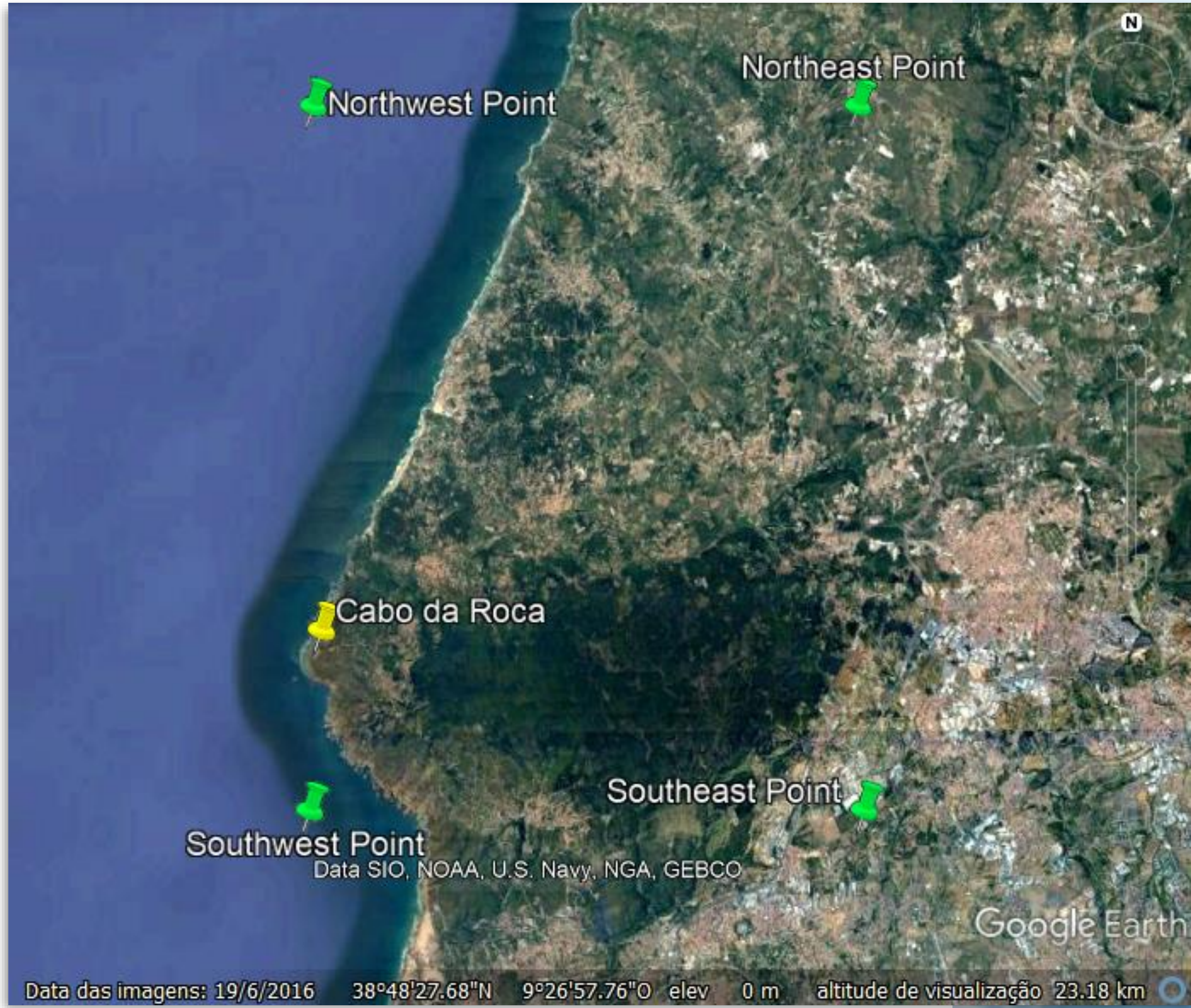
Northwest Point
Northeast Point
Cabo da Roca
Southeast Point
Southwest Point
Data SIO, NOAA, U.S. Navy, NGA, GEBCO
Google Earth
Data das imagens: 19/6/2016 38°48'27.68"N 9°26'57.76"O elev 0 m altitude de visualização 23.18 km

Influence of clearness index (K_t)

$$K_t = \frac{Predicted\ daily\ GHI}{Daily\ Irradiation\ on\ top\ of\ the\ atmosphere}$$

Hourly differences between predicted and measured GHI [J/m^2] as a function of daily K_t

Évora

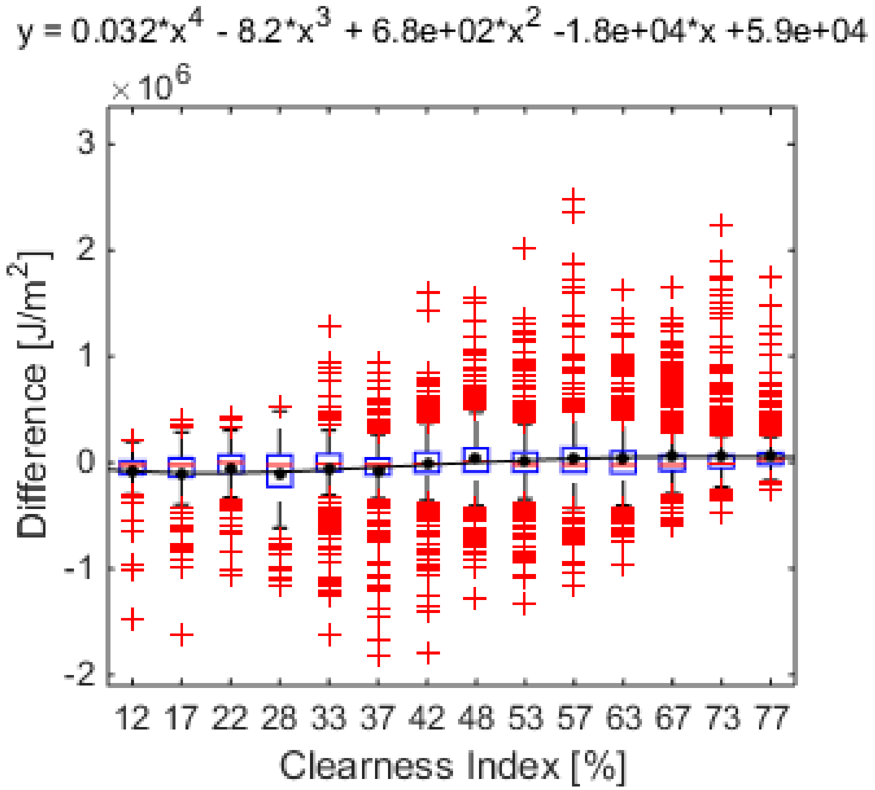

Sines

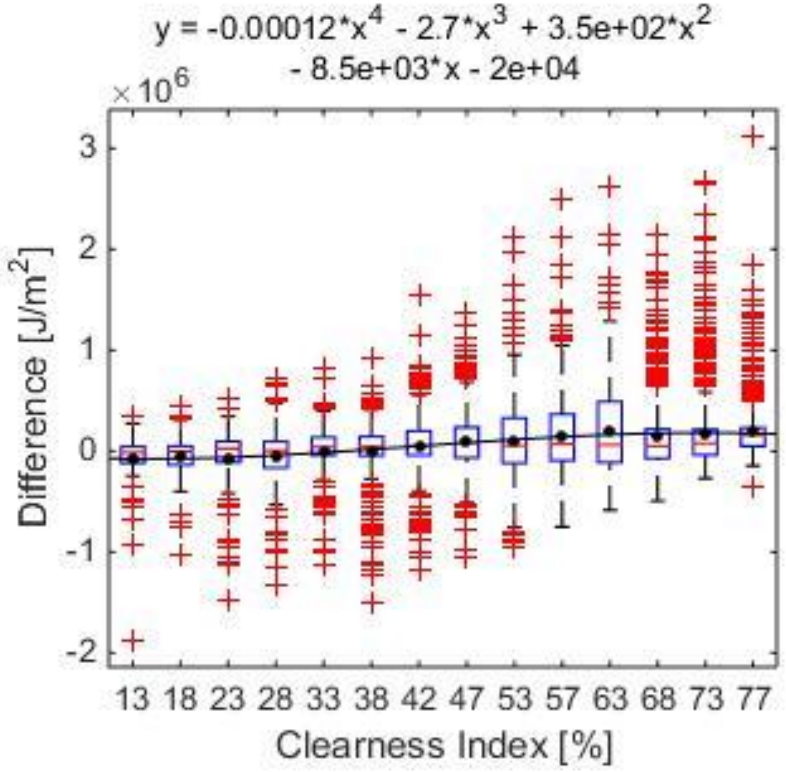

Influence of clearness index (K_t) and solar zenith angle

Average | Standard Deviation

Évora

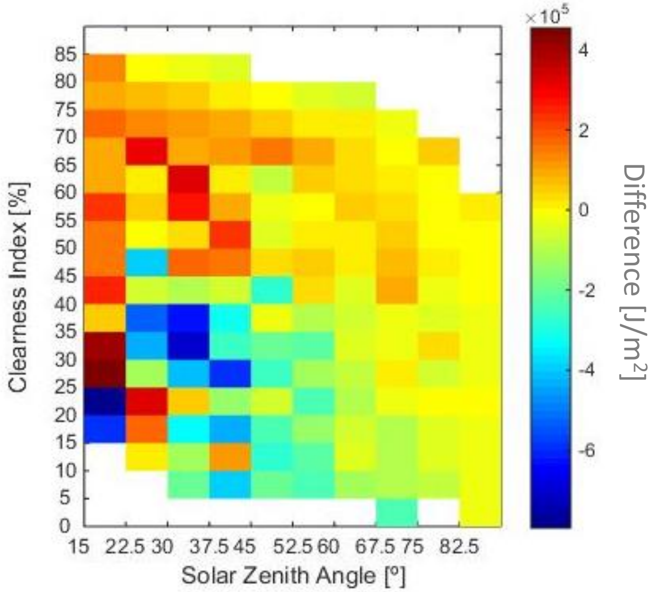

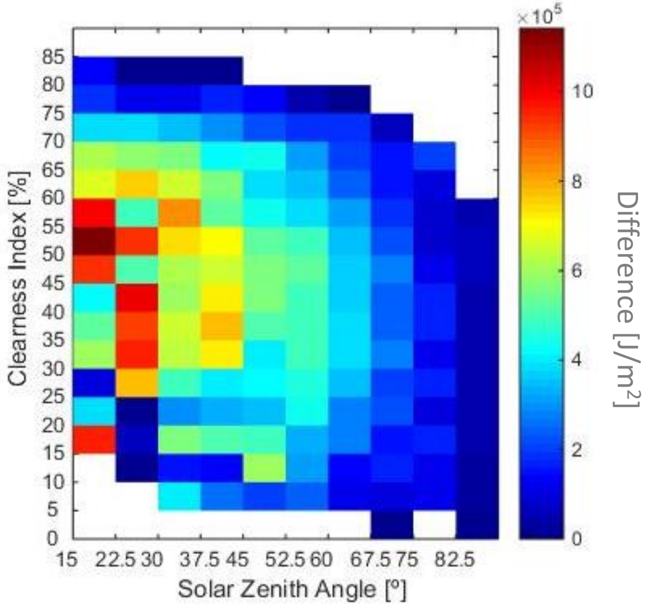

Sines

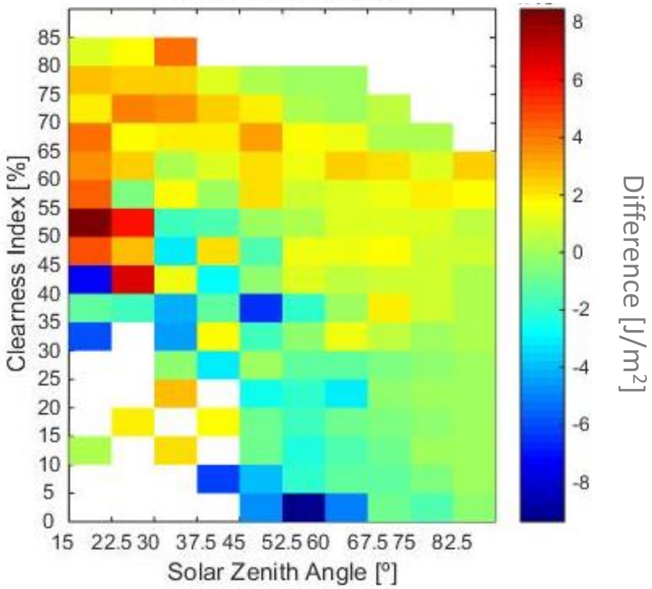

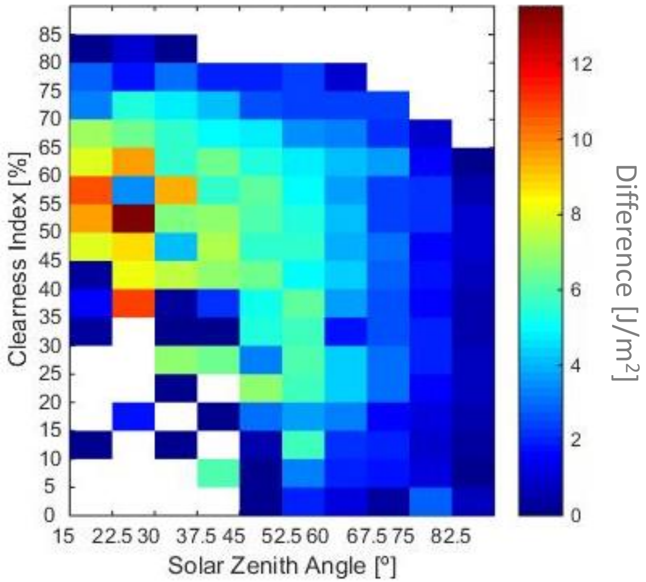

ICT
Instituto de Ciências da Terra
Institute of Earth Sciences

Influence of other variables

Mean Air Temperature | Relative Air Humidity | Total Water Column

Évora

Sines

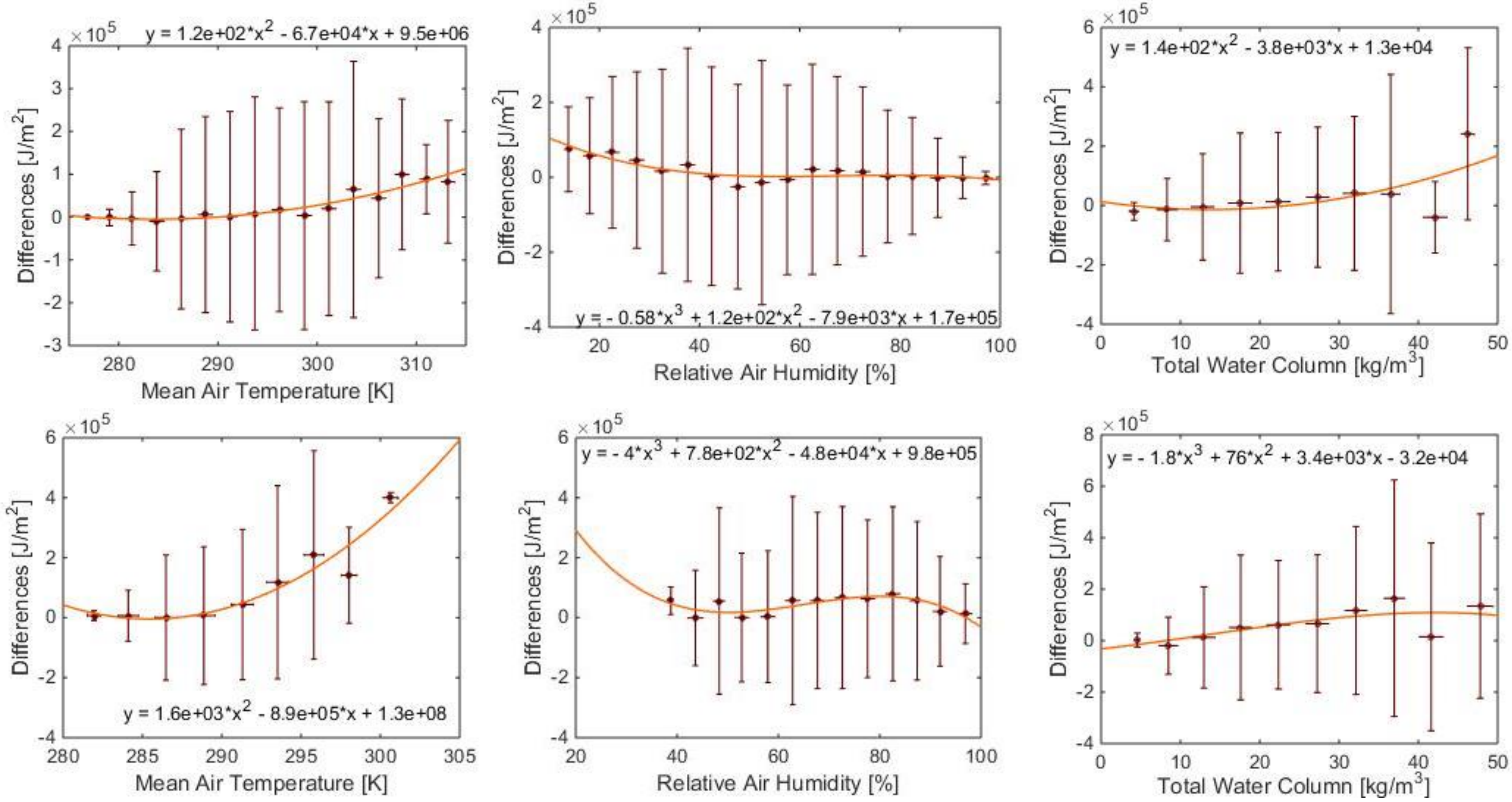

ANN development

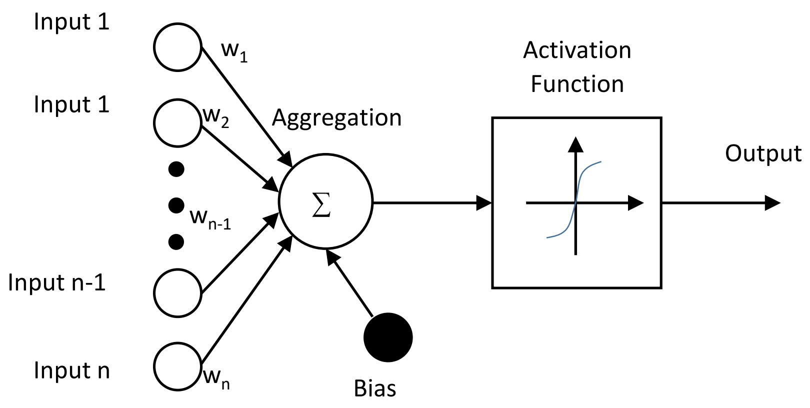

ANN parameters and inputs:

- Architecture: fitting network with 3 layers;
- Activation function: hyperbolic tangent sigmoid;
- Training function: Bayesian regulation backpropagation;
- 20 validation checks;
- 80% training, 20% validation.

- Common inputs: calculated solar radiation on top of the atmosphere, predicted GHI, visibility, cloud base height, total column water, total cloud cover, 10 meter wind velocity, 2 meter temperature, relative air humidity and total column ozone.

ANN development

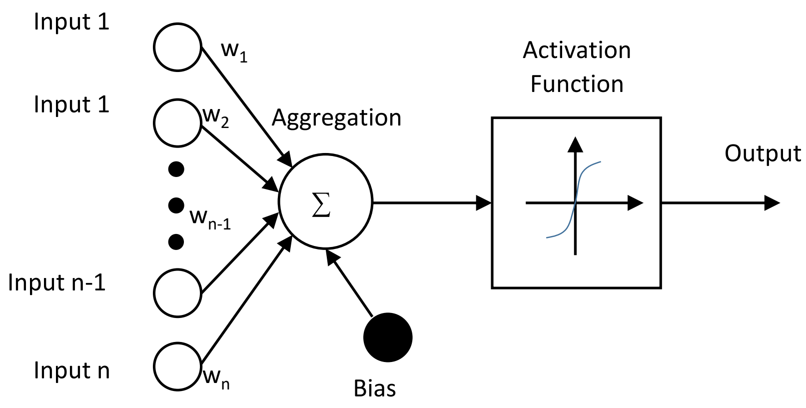

- Clear sky days ($K_t \geq 0.65$):
  - Additional inputs: GHI in clear sky conditions (ASHRAE), hour, day and month;
  - 58 neurons;
  - Deviation of 0.145 from clearness index.
- Partially cloudy days ($0.4 \leq K_t < 0.65$):
  - 30 neurons;
  - Deviation of 0.150 from clearness index.
- Overcast days ($K_t < 0.4$):
  - Additional inputs: GHI in clear sky conditions (ASHRAE);
  - 27 neurons;
  - Deviation of 0.145 from clearness index.

ANN development

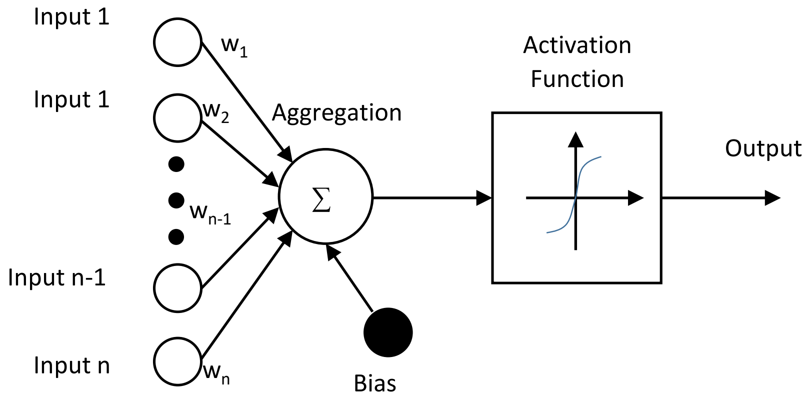

- Clear sky days ($K_t \geq 0.65$):
  - Additional inputs: GHI in clear sky conditions (ASHRAE), hour, day and month;
  - 58 neurons;
  - Deviation of 0.145 from clearness index.
- Partially cloudy days ($0.4 \leq K_t < 0.65$):
  - 30 neurons;
  - Deviation of 0.150 from clearness index.
- Overcast days ($K_t < 0.4$):
  - Additional inputs: GHI in clear sky conditions (ASHRAE);
  - 27 neurons;
  - Deviation of 0.145 from clearness index.

Test Results:

- Hourly average improvement of 22kJ/m^2;
- Hourly simulated values equal or closer to measurements than forecasts 61.84% of times.

Example

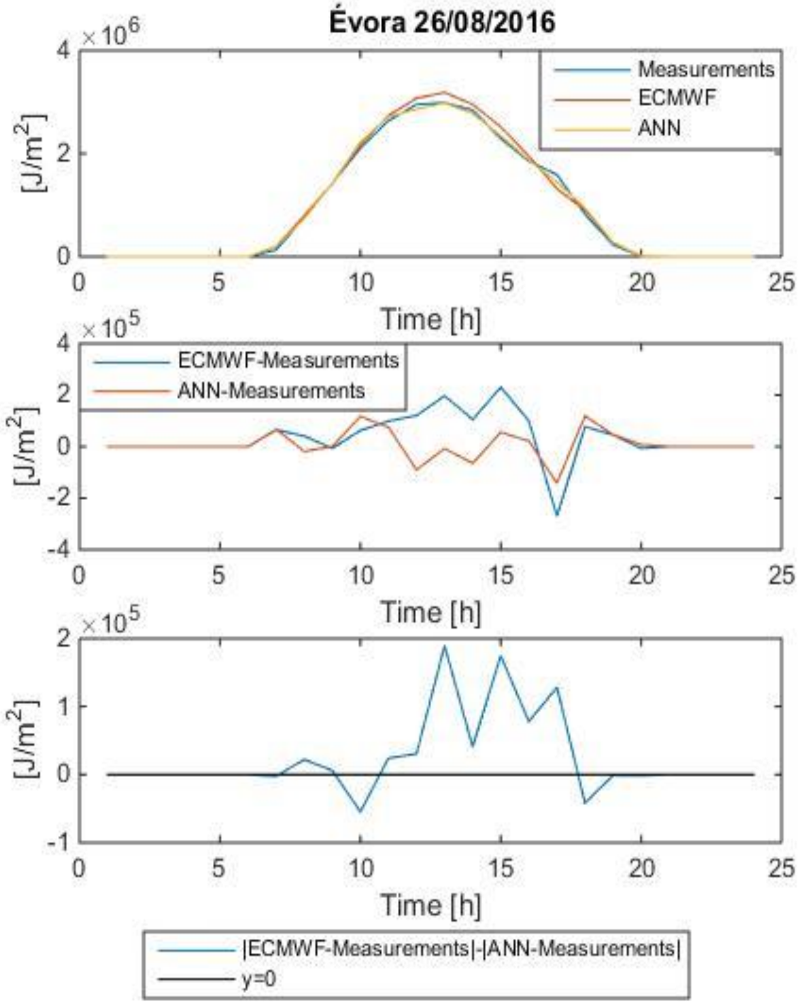

Évora 26/08/2016
Measurements
ECMWF
ANN
ECMWF-Measurements
ANN-Measurements
|ECMWF-Measurements|-|ANN-Measurements|
y=0
Time [h]
[J/m2]

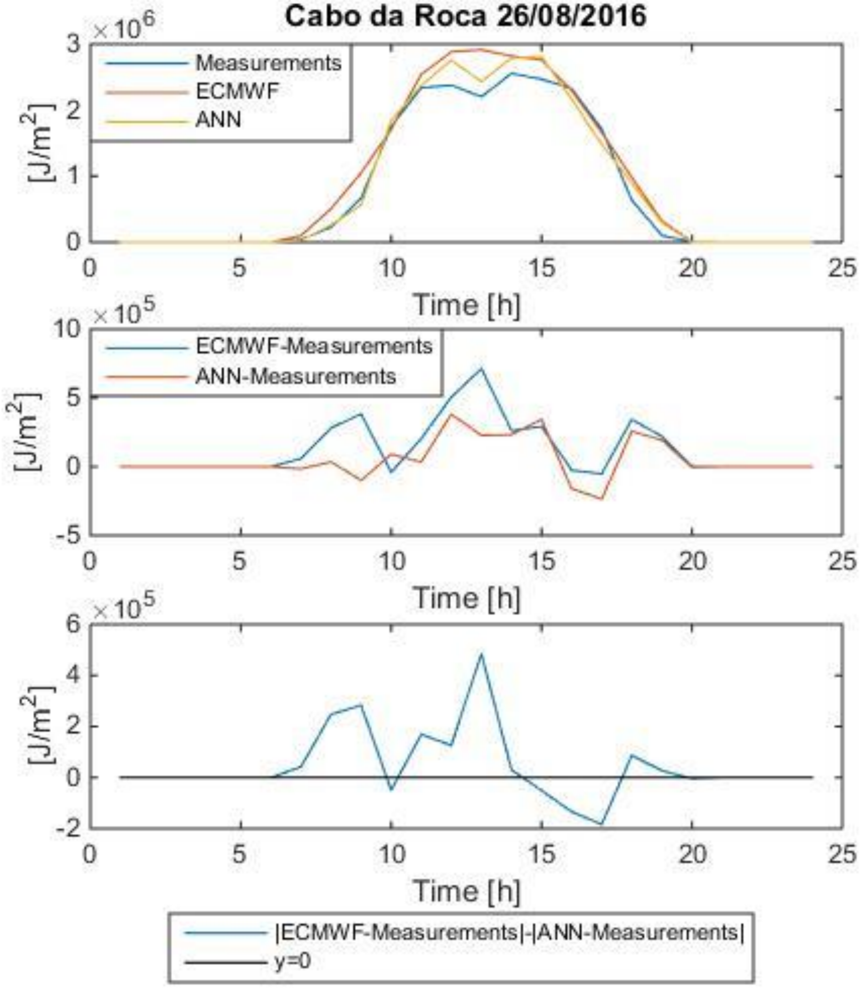

Cabo da Roca 26/08/2016
Measurements
ECMWF
ANN
ECMWF-Measurements
ANN-Measurements
|ECMWF-Measurements|-|ANN-Measurements|
y=0
Time [h]
[J/m2]

Conclusion

- Influence of atmospheric and Sun-Earth geometry related variables in the differences between predictions and measurements of GHI:
    - Clearness index;
    - Zenith angle;
    - Mean air temperature;
    - Relative air humidity;
    - Total column water.

- Development of a corrective ANN:
    - Average hourly improvement of 22 kJ/m^2;
    - Simulations equal or better than forecasts 61.84% of the times.

This algorithm will be integrated in a more complete model, a global solar radiation and mean air temperature prediction algorithm that will be used in energy management in medium/low temperature solar thermal systems. It is expected that the integration of the algorithm in these types of models or models of other solar energy conversion units, will allow for a better management of renewable energy conversion and a better design and usage of conventional auxiliary systems.

Thank you!

Acknowledgment

This work was carried out under the contract with the company Warmhole, lda for the development of a solar radiation forecast algorithm. The authors wish to acknowledge ECMWF and IPMA for the provision of data and the funding provided by the European Regional Development Fund, included in the COMPETE 2020 (Operational Program Competitiveness and Internationalization) through the ICT project (UID/GEO/ 04683/2013) with the reference POCI-01-0145-FEDER -007690, DNI-A (ALT20-03-0145-FEDER-000011) and ALOP (ALT20-03-0145-FEDER-000004) projects .